NREL
NATIONAL RENEWABLE ENERGY LABORATORY

Assessment and Optimization of Lidar Measurement Availability for Wind Turbine Control

Preprint

S. Davoust, A. Jehu, M. Bouillet, M. Bardon, and B. Vercherin
Avent Lidar Technology

A. Scholbrock, P. Fleming, and A. Wright
National Renewable Energy Laboratory

Presented at EWEA 2014
Barcelona, Spain
March 10–13, 2014

NREL is a national laboratory of the U.S. Department of Energy
Office of Energy Efficiency & Renewable Energy
Operated by the Alliance for Sustainable Energy, LLC

This report is available at no cost from the National Renewable Energy Laboratory (NREL) at www.nrel.gov/publications.

Conference Paper
NREL/CP-5000-61332
May 2014

Contract No. DE-AC36-08GO28308

This report is available at no cost from the National Renewable Energy Laboratory (NREL) at www.nrel.gov/publications.

Available electronically at http://www.osti.gov/scitech

Available for a processing fee to U.S. Department of Energy and its contractors, in paper, from:

U.S. Department of Energy
Office of Scientific and Technical Information
P.O. Box 62
Oak Ridge, TN 37831-0062
phone: 865.576.8401
fax: 865.576.5728
email: mailto:reports@adonis.osti.gov

Available for sale to the public, in paper, from:

U.S. Department of Commerce
National Technical Information Service
5285 Port Royal Road
Springfield, VA 22161
phone: 800.553.6847
fax: 703.605.6900
email: orders@ntis.fedworld.gov
online ordering: http://www.ntis.gov/help/ordermethods.aspx

Cover Photos: (left to right) photo by Pat Corkery, NREL 16416, photo from SunEdison, NREL 17423, photo by Pat Corkery, NREL 16560, photo by Dennis Schroeder, NREL 17613, photo by Dean Armstrong, NREL 17436, photo by Pat Corkery, NREL 17721.

Printed on paper containing at least 50% wastepaper, including 10% post consumer waste.

Assessment and Optimization of Lidar Measurement Availability for Wind Turbine Control

Samuel Davoust[1*], Alban Jehu[1], Michael Bouillet[1], Mathieu Bardon[1], Benoist Vercherin[1], Andrew Scholbrock[2], Paul Fleming[2], and Alan Wright[2]

1: Avent Lidar Technology, Orsay, France
2: *National Renewable Energy Laboratory, Boulder, CO, USA*
**Avent Lidar Technology, 3 rue Jean Rostand, 91400 Orsay, France; email: sdavoust@aventlidar.com*

Abstract

Turbine-mounted lidars provide preview measurements of the incoming wind field. By reducing loads on critical components and increasing the potential power extracted from the wind, the performance of wind turbine controllers can be improved [2]. As a result, integrating a light detection and ranging (lidar) system has the potential to lower the cost of wind energy. This paper presents an evaluation of turbine-mounted lidar availability. Availability is a metric which measures the proportion of time the lidar is producing controller-usable data, and is essential when a wind turbine controller relies on a lidar. To accomplish this, researchers from Avent Lidar Technology and the National Renewable Energy Laboratory first assessed and modeled the effect of extreme atmospheric events. This shows how a multirange lidar delivers measurements for a wide variety of conditions. Second, by using a theoretical approach and conducting an analysis of field feedback, we investigated the effects of the lidar setup on the wind turbine. This helps determine the optimal lidar mounting position at the back of the nacelle, and establishes a relationship between availability, turbine rpm, and lidar sampling time. Lastly, we considered the role of the wind field reconstruction strategies and the turbine controller on the definition and performance of a lidar's measurement availability.

1. Introduction

Integrating light detection and ranging (lidar) technology to improve wind turbine controls is a potential breakthrough for reducing the cost of wind energy [1]. By providing undisturbed wind measurements up to 400 m in front of the rotor, turbine-mounted lidars provide an accurate update of the turbine inflow with a preview time of several seconds. Several studies have evaluated potential reductions in loads using integrated lidar, either by simulation [2, 3] or full-scale field testing [4, 5]. Leading wind turbine manufacturers have also started to evaluate the technology [6]. From a business standpoint, one of the key aspects that should be validated is the availability of lidar measurements; if the lidar is not delivering measurements, benefits cannot be obtained.

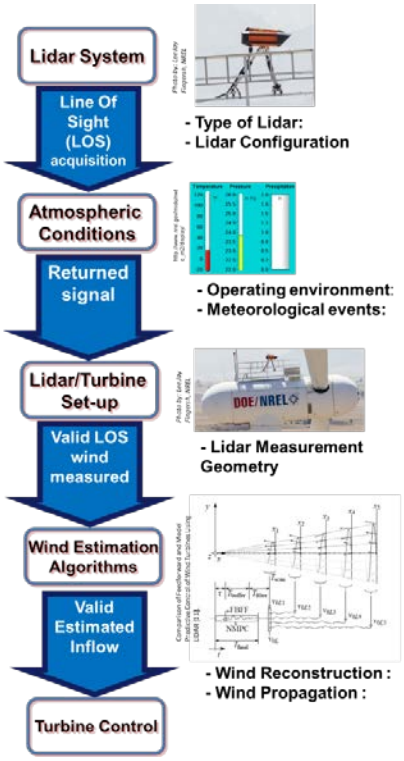

Figure 1: Schematic of lidar measurement process for wind turbine control.

The present work provides an overview of the measurement availability that can be achieved with a turbine-mounted lidar, and describes methods to optimize lidar integration for turbine control. Availability can be generally defined as the percentage of valid "wind estimations" obtained over a given period of time. The measurement process for a lidar has now been described in [7].

As depicted in Figure 1, the key parameters governing measurement availability with a turbine-mounted lidar are the atmospheric conditions, the lidar configuration on the wind turbine, and the wind field estimation algorithm.

2. Problem

Lidar systems acquire signals along one or several lines of sight (beams). The measurement which is derived is a projected wind speed along the line-of-sight (LOS). The average availability of wind measurements along a line of sight can be defined as the ratio of valid LOS measurements over the total number of measurements expected within a specified period. In the following discussion, this parameter will be defined as A_{LOS}. When the lidar beam propagates freely in the atmosphere, A_{LOS} is a function of the type of lidar system used, the lidar measurement configuration (e.g., sampling rate and range), and of the atmosphere encountered.

As shown in Figure 1, the lidar mounting position on the turbine can affect the line-of-sight (LOS) measurement. The main impacts on the lidar measurement from the turbine can be a periodic lidar motion (e.g., oscillation or rotation), or a periodic blade passage in front of the lidar beams. These effects could impact the LOS availability so we denote it as A_{LOS}^{T} in the turbine-mounted configuration. The difference between A_{LOS} and A_{LOS}^{T} may also depend on the type of lidar technology used, and it is expected that $A_{LOS}^{T} < A_{LOS}$.

LOS measurements are reconstructed into an effective signal such as a rotor-averaged wind speed [8] and used by the turbine controller as feedforward input of the wind field. This leads to defining a validity rule with respect to the number of LOS measurements necessary (i.e., distance and time) to build this effective signal. This definition may depend on the type of measurements available (e.g., single range or multiple ranges). The choice of one definition thus results in an effective availability noted as A_E that could be greater or less than A_{LOS} or A_{LOS}^{T}. Design of the definition for a specific lidar and turbine controller technology may be required.

In this paper, the sensitivity of lidar availability from external parameters is investigated and modeled for each step. Operational feedback from a lidar system installed at the National Renewable Energy Laboratory (NREL) test site in Boulder, Colorado, and data collected from over 20 additional turbine-mounted lidars deployed in several configurations is used to verify the analyses.

3. Effects of atmospheric conditions on availability

In regular atmospheric conditions, lidars are designed to deliver 100% LOS measurement availability across all specified ranges. However, under specific conditions, a lidar measurement can become unavailable at a specific range if the returned signal is not strong enough or does not match quality filters. Thus, verifying the availability of measurements within a specified measurement range is central to the control application because range determines the prediction time for the turbine. The carrier-to-noise ratio (CNR) is one of the main parameters that can be used to flag lidar wind measurements as valid [7].

3.1. Simulation of lidar signal in different atmospheric conditions

To understand the behavior of average CNR, we performed a theoretical computation of the lidar signal using an in-house lidar simulation tool that was previously validated [7]. The main parameters of the computation are the atmospheric transmission (α) and backscattering (β) coefficients on the one hand, and the choice of lidar components on the other. For this study, the parameters used in the simulation were set to the same parameter values that were used on a Wind Iris lidar that was mounted on a wind turbine at the National Wind Technology Center at NREL. The atmospheric backscatter coefficient was varied from 10^{-3} (extreme fog) to 10^{-8} (higher than normal, or very high visibility) and a hypothesis was made for the transmission coefficient (α=βx40). The results are provided in Figure 2.

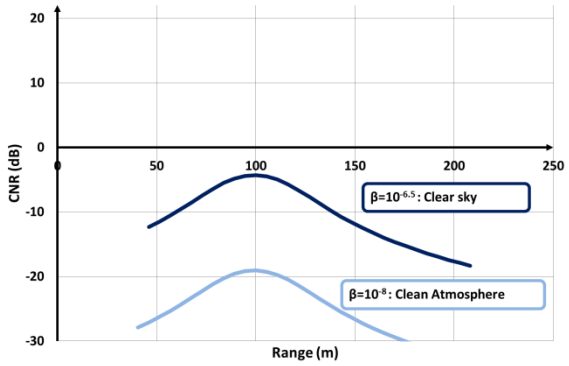

Figure 2 (a): Simulation of lidar system CNR in good visibility. The upper curve corresponds to "normal visibility". The lower curve corresponds to a "very high visibility" case.

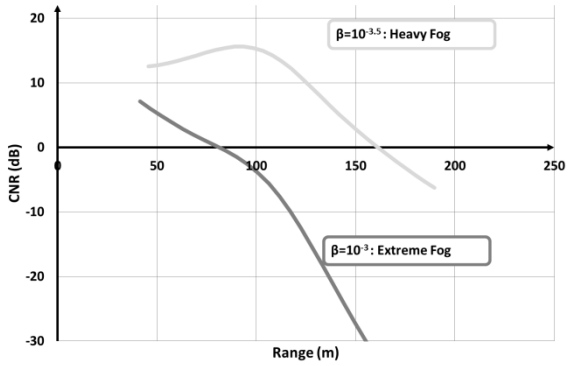

Figure 2 (b): Simulation of lidar system CNR in a fog situation. The upper curve corresponds to "Heavy Fog". The lower curve corresponds to an "Extreme Fog" situation.

Under normal visibility, Figure 2(a) shows that the current setup should provide a slightly peaked CNR around 100 m. If visibility increases from being "normal" to "very high," the concentration of aerosol particles, which reflect the lidar signal, decreases. As can be seen in Figure 2(a), this effect should cause CNR to globally decrease, which could lead to a reduced availability at close and long range. In foggy conditions, Figure 2(b) shows that the CNR curve should have a different shape, with a much stronger initial CNR signal, followed by a faster decrease. This effect can be explained by the fact that fog is a suspension of micro-water-droplets, thereby providing a stronger reflective signal at close range, but at the same time scattering the laser energy at greater distances, leading to a faster drop of CNR. In extreme fog, the concentration of water droplets is higher: as a result a stronger reflection and CNR should be observed at close range but as the light will diffuse quicker at longer range, thus the rate of CNR decrease might increase.

3.2. Observations and analysis of experimental data

We performed an analysis of lidar LOS availability under various atmospheric conditions. Over the course of a 6-month campaign, a Wind Iris lidar was installed on the NREL two-bladed Controls Advanced Research Turbine (CART2) located in Boulder, Colorado, at 1,855 m altitude, as shown in Figure 1. This pulsed lidar measures 10 ranges at 2 Hz and its optics are focused around 100 m to ensure an optimal availability from 50 m to 150 m. For this lidar system, the min/max CNR rule was set to (-19 dB, +10 dB). Using a webcam located at 100 m from the turbine and other instrumentation, we created weather categories to investigate lidar availability in clear sky, heavy rain, snow, or fog. Periods where the turbine was stopped were identified to compute A_{LOS}, independently of lidar/turbine interactions.

Figure 3 provides examples that show the performance of a commercial lidar dedicated to close range measurements (40 m to 200 m). Under nominal conditions (normal visibility), A_{LOS} is constant and near 100%, but starts to decrease beyond 160 m. During the heavy rain event, 7 mm of precipitations was recorded in 10 minutes (30 mm fell within 1 hour). A_{LOS} is observed to be maintained, and even increased in the farthest ranges, suggesting that rain does not itself reduce availability. Degradation of availability is, however, observed during a snow event. Nevertheless, the CNR average is maintained around -15 dB at around 100 m, providing nearly 100% of availability at this range. In heavy fog (visibility below 50 m), CNR strongly increases at close range, but availability is lower at 50 m than at 200 m. The fact that availability is lower while the CNR is high is explained by a factory +10 dB CNR upper limit. It should be assessed whether this upper limit should be removed for turbine control applications.

The experimental CNR findings agree well with the simulations for good visibility and heavy fog cases and confirm that, with proper lidar system design, strategies could be developed to deliver measurements even in very difficult atmospheric conditions. However, Figure 3 also shows that the min/max CNR amplitude varies as a function of atmospheric conditions. As a result, we recommend investigating the statistical distribution of CNR when planning a field campaign. Indeed, even if the average CNR implies valid measurement, a large dispersion that brings some CNR values below the threshold could reduce availability.

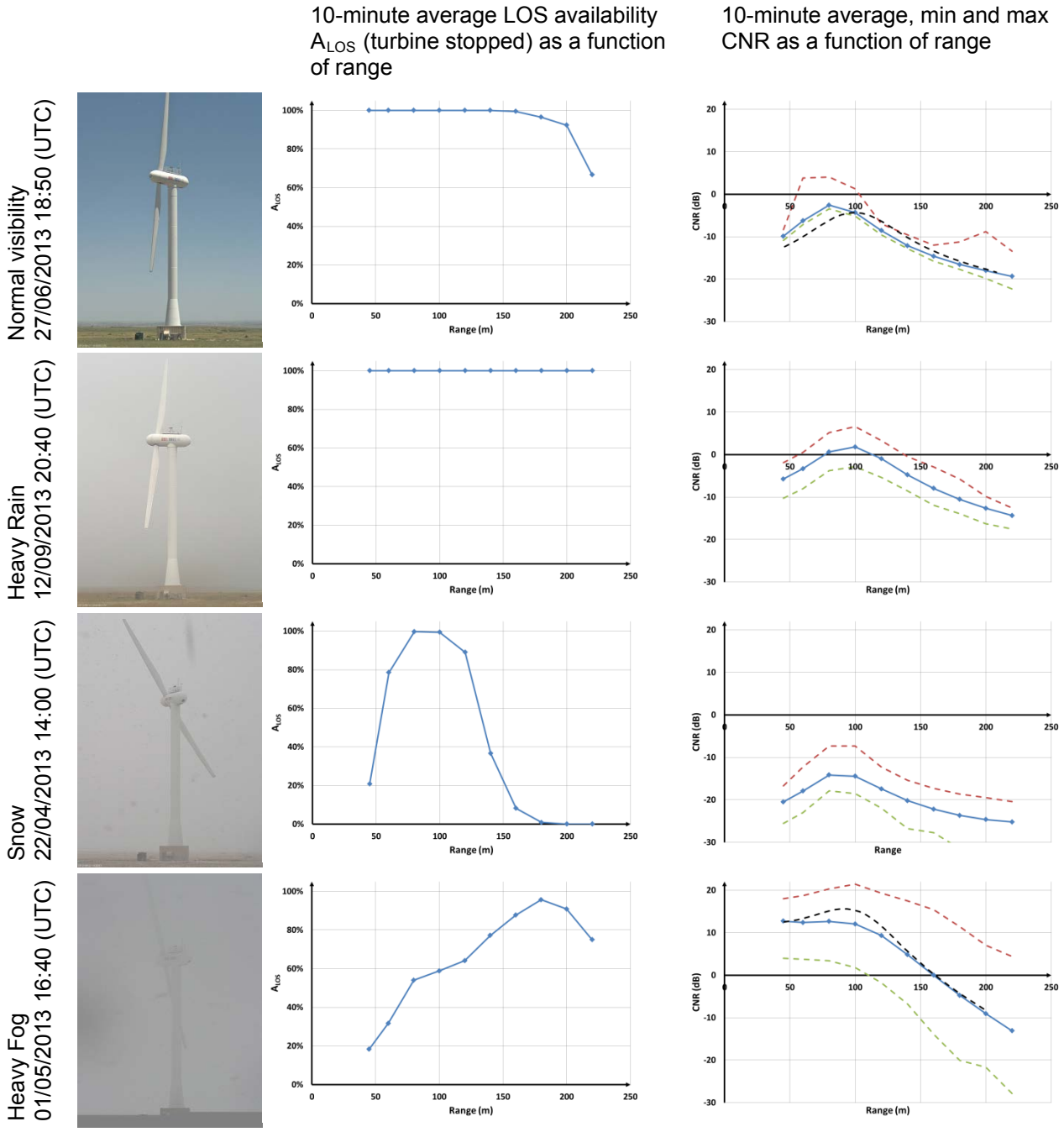

Figure 3 : Atmospheric conditions experienced over a 10-minute period, field pictures, lidar system average availability A_{LOS}, and 10-minute **average**, **min**, and **max** Carrier-to-Noise Ratio (CNR) as a function of range. The **dashed black line** reproduces the CNR simulated in Figure 2a (good visibility) and 2b (heavy fog) for reference.

4. Availability behavior according to lidar/turbine setup

In this section, we focus on the availability impact of the lidar geometry and mounting position on the wind turbine. For instance, different mounting positions have an effect on availability because of the interference between the lidar laser signal and the turbine's blades. The lidar can be mounted at various heights on the turbine nacelle, such as just behind the rotor or at the back of the nacelle, as shown in Figure 4 (a). However, because the turbine's blades can interfere with the lidar's laser beams, special consideration is needed to ensure

that blade passing does not affect the wind measurement. For a pulsed lidar, the signal reflected by a blade does not contribute to measurements because the time of flight for the return signal does not match that of upstream measurements, and is therefore rejected. Another possibility is to install the lidar system inside the turbine's spinner [9], which has the advantage of removing the blade interference but may require a more complex mechanical integration, and data transfer and processing system.

4.1. Evaluation of signal availability from average geometrical blocking

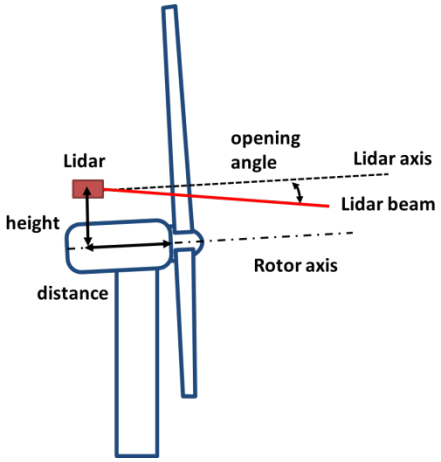

Figure 4 (a): Schematic representation of a lidar system at the back of a wind turbine's nacelle.

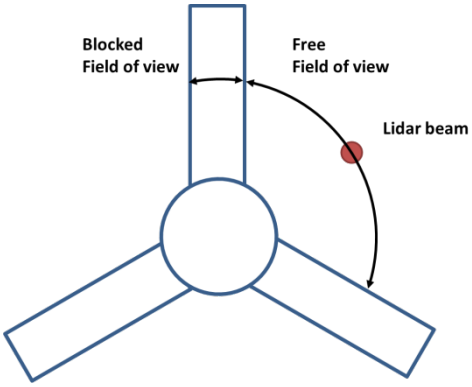

Figure 4 (b): Schematic representation of the position of the lidar beam in the rotor plane.

The first parameter that should govern turbine-mounted lidar measurement availability $A_{LOS}{}^{T}$ is the percentage of average available field of view allowed by the rotor, as noted by Δ. As shown in Figure 4 (b), it can be computed as the ratio between the sum of the three blades' root diameter ($3\ d_L$) and the rotor circumference at the local radius where a lidar beam intersects with the blades ($2\ \pi\ R_L$). This ratio is given by Eq. 1:

$$\Delta = 1 - \frac{3d_L}{2\pi R_L} \quad (1)$$

Assuming a 2.5-m blade root diameter, Figures 5 (a) and (b) show the evolution of Δ as a function of the lidar system distance behind the rotor, considering different lidar beam opening angles (α) and heights (h) above the rotor axis. Figure 5 (a) and (b) shows that bringing the lidar to the back of the nacelle and raising it above the hub both improve Δ. Similarly, a wider beam opening angle also improves availability, especially as the lidar is moved back on the nacelle. These theoretical results are in line with field observations on over 20 documented turbine lidar installations on various nacelle types from 1.5-MW to 7.5-MW turbines, where this parameter varied from 50% to 80%.

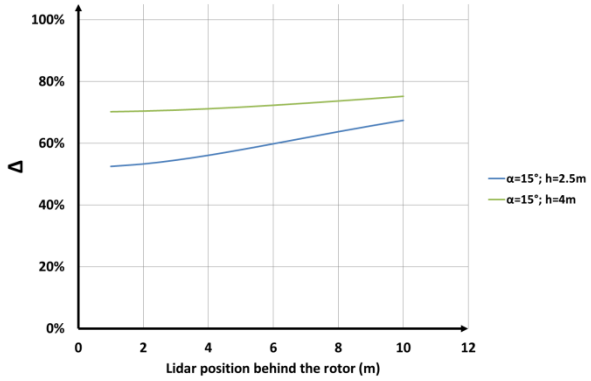

Figure 5 (a): Available field of view Δ as a function of lidar system distance behind the rotor for two heights above the rotor axis and a beam opening angle of 15°.

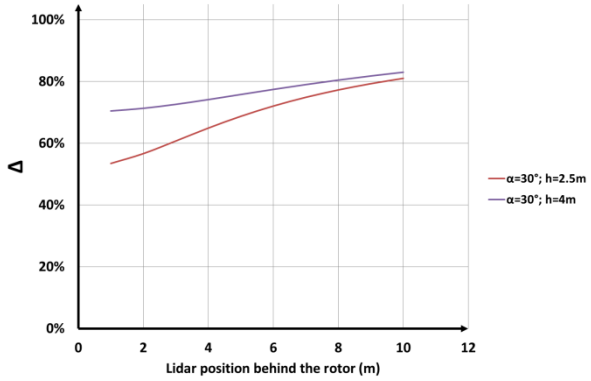

Figure 5 (b): Available field of view Δ as a function of lidar system distance behind the rotor for two heights above the rotor axis and a beam opening angle of 30°.

4.2. Evolution of lidar signal availability with temporal blocking effect

Temporal parameters such as the lidar measurement integration time (σ) and the rotor rotation speed (rpm) also have an effect on A_{LOS}^{T}. Indeed, Figure 6 shows an example of the lidar signal availability along one beam as a function of rotor rpm speed. For low rpm, the figure shows that availability is near 65%, which is the valid field of view Δ, but reaches 100% when rpm is above 80% of turbine rated speed. This dependence with rotor rpm can be explained by the temporal nature of the measurement process. In fact, we show below that Δ sets the upper bound to measurement availability at a very low rpm, while the upper bound to measurement availability of a high rpm depends on a time scale ratio between the lidar signal acquisition time and the blade passage period.

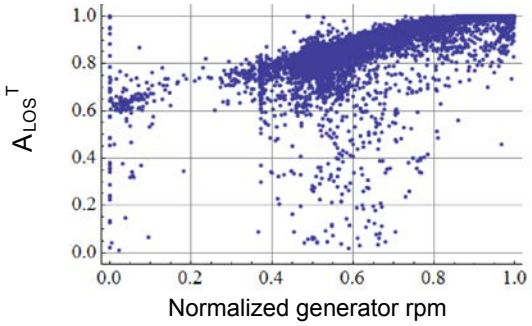

Figure 6: Example of Lidar beam availability as a function of normalized generator rpm [9].

For modern wind turbines, the rotor speed varies between 3 rpm and 18 rpm [10], while lidar signal integration time can vary from 1 Hz to 50 Hz [7]. For a low rotor speed (say below 5 rpm), the blade passage will tend to last longer than the lidar signal integration time. As a result, a blade can completely block a measurement. In this case, the percentage of data loss is equal to the percentage of time a blade is in front of a beam, which is exactly 1-Δ.

However, for a faster speed (say above 10 rpm), the blade passage time will tend to become lower than the Lidar acquisition time. In this case, depending on the lidar technology used, the lidar measurement may still be valid despite the blade partially blocking the beam. The ratio between the lidar signal integration time (σ) and the time taken for a blade to pass completely in front of a beam can be written as:

$$\Sigma = \sigma \frac{rpm}{60} \frac{3}{1-\Delta} \quad (2)$$

If this parameter becomes greater than one, it means the lidar can always "see through the blade" and completely gain back the availability lost (given by 1-Δ). Σ = 0 corresponds to the low rotor speed case where the Lidar availability is Δ as described above. If Σ is between 0 and 1, a part of the 1- Δ availability loss can be recovered. This recovered part is governed by the amount of CNR decrease due to a partial obstruction. As CNR is measured as a decimal logarithm scale, when a blade obstruction divides the acquisition time by 2, this removes 3 dB of CNR. In operational conditions, the validity of a LOS measurement will be kept as long as after the CNR loss, the CNR remains above the threshold.

As a first model, it can be roughly assumed that availability loss is inversely proportional to Σ. In this case, lidar signal availability should be estimated by:

$$A_{LOS}^{T} = \begin{cases} \Delta + \Sigma\,(1-\Delta) & if\ \Sigma < 1 \\ 1 & if\ \Sigma \geq 1 \end{cases} \quad (3)$$

To evaluate this model, researchers investigated availability using average lidar data from 20 different turbine-mounted configurations. This evaluation allowed us to cover various lidar signal-sampling rates and turbine rpm configurations, as well as cases where the lidar was in the back or front of the nacelle. Furthermore, this evaluation generates a wide range for parameters Σ and Δ, as shown in Figure 7 (a).

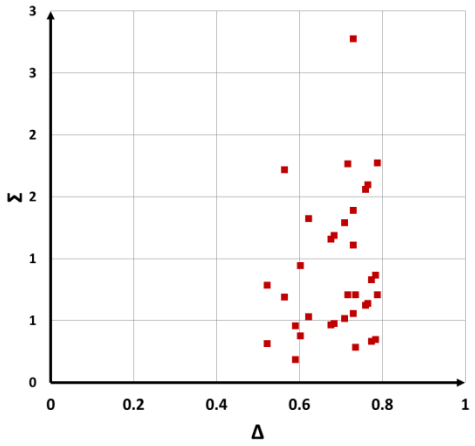

Figure 7(a): Map of the lidar system field-of-view Δ and lidar-to-blade time ratio Σ observed over 20 different turbine-mounted lidar system configurations.

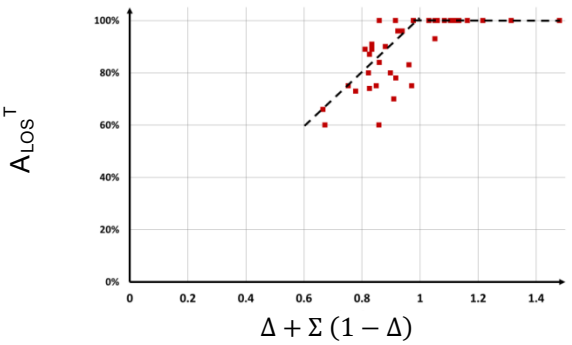

Figure 7(b): Corresponding correlation between measured lidar signal availability (red squares) and estimated availability parameter according to eq. 3 (dashed line) as a function of Δ + Σ(1- Δ).

In turn, Figure 7 (b) shows a good correlation between measured availability and estimated availability, thereby confirming the approach used with the above model with the existence of two regimes. When Σ is much smaller than 1, the lidar signal availability is governed by Δ, the available field of view. When Σ is larger than 1, the lidar signal availability should be 100%. This model should help determine which lidar configuration best suits measurement requirements. A next step would be to refine the model according to realistic CNR distribution with range such as depicted in Figure 3, combined with a CNR loss which is dependent to blade obstruction time.

5. Effect of real-time wind field reconstruction algorithm

We have shown that LOS signal availability can be modeled simply. Although this topic is still being investigated, it is worth noting that from a wind turbine control point of view, only reconstructed wind parameters estimated using several lidar beams or ranges should be used. For instance, using measurements that are available across all lidar measurement ranges can improve the estimation of wind parameters. The validity of wind estimation then depends on the minimum number of ranges and points required during a specific time interval, according to the wind turbine control requirements. Thus, the lidar system availability performance should be evaluated according to this metric.

6. Conclusion

We investigated the measurement availability of turbine-mounted lidar systems for a wide range of parameters including lidar system characteristics, mounting configurations, atmospheric conditions, and wind reconstruction algorithms. We demonstrated that the main effects of these parameters can be modeled and predicted, and established several aspects that contribute to the definition and performance of lidar availability for wind turbine control. We obtained promising results in various atmospheric conditions.

In this paper, we provide a critical analysis of availability performance with respect to turbine control application, and propose optimization strategies to remedy cases of low performance. Further work and collaboration between research teams, and lidar and turbine manufacturers is required to validate this approach, which can then strengthen the value behind integrating lidar systems into the next generation of turbines.

References

[1] A. Byrne, T. McCoy, K. Briggs, T. Rogers. “Expected Impacts on Cost of Energy through Lidar Based Wind Turbine Control.” European Wind Energy Association Conference, Copenhagen, Denmark, 2012.

[2] E. A. Bossanyi, A. Kumar, O. Hugues-Salas. “Wind turbine control applications of turbine-mounted LIDAR.” Torque from Wind Conference, Oldenburg, Germany, 2012.

[3] C. L. Bottasso, F. P. Pietro Pizzinelli, C. E. D. Riboldi. “Lidar-enabled real-time control of wind turbines.” European Wind Energy Association Conference, Vienna, Austria, 2013.

[4] D. Schlipf, P. Fleming, F. Haizmann, A. Scholbrock, M. Hofäß, A. Wright, P. W. Cheng. “Field Testing of Feed forward Collective Pitch Control on the CART2 Using a Nacelle-Based Lidar Scanner.” Torque from Wind conference, Oldenburg, Germany, 2012.

[5] A. Scholbrock, P. Fleming, L. Fingersh, A. Wright,D. Schlipf, F. Haizmann, F. Belen. “Field testing LIDAR based feed-forward controls on the NREL controls advanced research turbine.” 51st AIAA Aerospace Sciences Meeting Including the New Horizons Forum and Aerospace Exposition, Grapevine, Texas, 2013.

[6] A. Koerber, C. Mehendale. “Lidar Assisted Turbine Control...An Industrial Perspective.” American Wind Energy Association Conference, Chicago, USA, 2013.

[7] J. P. Cariou, M. Boquet. “LEOSPHERE Pulsed Lidar Principles.” UpWind WP6 report on Remote Sensing Devices. 2010.

[8] D. Schlipf, L. Y. Pao, and P. W. Cheng. “Comparison of Feed-Forward and Model Predictive Control of Wind Turbines Using LIDAR.” Proceedings of the Conference on Decision and Control, Maui, USA, 2012.

[9] T. Mikkelsen, N. Angelou, K. H. Hansen, M. Sjöholm, M. Harris, C. Slinger, P. Hadley, R. Scullion, G. Ellis, G. Vives. “A spinner-integrated wind Lidar for enhanced wind turbine control.” Wind Energy, Vol. 16, 2013, p. 625–643.

[10] R. Wagner, S. Davoust. “Nacelle lidar for power curve measurement _ Avedøre campaign.” DTU Wind Energy E-0016, 2013.

[11] A. D. Hansen, F. Iov, F. Blaabjerg, L. Hansen. “Review of contemporary wind turbine concepts and their market penetration.” Wind Engineering, Vol. 28, No. 3, 2004.